A novel integral principle for evaluating 3D weakly singular boundary integrals

Yudong Zhong, Jianming Zhang*, Yunqiao Dong, Yuan Li

(State Key Laboratory of Advanced Design and Manufacturing for Vehicle Body, Hunan University, Changsha 410082, China)

*Correspondence to: Jianming Zhang

College of Mechanical and Vehicle Engineering, Hunan University, Changsha 410082, China

Telephone: +86-731-88823061

E-mail: zhangjianm@gmail.com

ABSTRACT

A novel integral principle is presented in this paper for evaluating weakly singular boundary integrals. Accurate and efficient evaluation of weakly singular integrals arising in the boundary integral equations (BIEs) is of crucial importance for successful implementation of the boundary element method (BEM). Various methods have been proposed to cope with these integrals. Element subdivision is one of the most widely used methods for the numerical evaluation of weakly singular integrals. Through the element subdivision, an element is subdivided into a number of patches by a sequence of spheres centered at the source point. In our method, an improved serendipity triangle patch with four-node is obtained through the element subdivision. One edge of the patch we obtained is replaced by quadratic curve, which is different from the traditional patch. In the serendipity patch, the distance between the middle node of the quadratic curve and the source point is equal to the length of radius of the sphere which is centered at the source point. Furthermore, in order to investigate the effect of the location of the middle node on the accuracy of integral, we have changed its location along the direction of the middle node to the source point step by step. Through theoretical deduction and numerical experiment, the location with the highest accuracy has been found in this paper. Moreover, the coordinate transformation is used to evaluate the weakly singular integral in the serendipity triangle patch and the Gaussian points distribute in the radial pattern. Comparing with the conventional method, our method can achieve higher accuracy by smaller number of Gaussian points, especially for the large-angle patch. Numerical examples are presented to verify the proposed method. Results demonstrate the accuracy and efficiency of our method.

Keywords: *BIEs, BEM, weakly singular integral, four-node isosceles triangle patch, Gaussian quadrature.*

1. Introduction

Weakly singular integrals are appeared in the basic boundary integral equations (BIEs) when the boundary integral equation method (BEM) is used to solve potential and mechanical problems. There are many ways of evaluating weakly singular integrals mentioned in the boundary element literature. These approaches include integral simplification [1], element subdivision [2] and coordinate transformation [3]. Moreover, polar coordinate transformation is a powerful and useful tool to evaluate weakly singular integral in boundary element. It converses the surface integral into a double integral in radial and angular directions. Many works have been done on dealing with the singularity in the radial direction; however, numerical integration on the angular direction still deserves more attention. In fact, after singularity cancelation or subtraction, although the integrand may behave very well in the radial direction, its behavior in the angular direction would be much worst, so too many quadrature points are needed. Especially when the source point lies close to the boundary of the element, one can clearly observe near singularity of the integrand in the angular direction. Similar problems have been considered in work about the nearly singular BEM integrals. Effective methods along this line are the subdivision method [4], the Hayami transformation [5], the sigmoidal transformation [6], the conformal transformation [7], the variable transformation [8], etc.

In this paper, Sphere subdivision method proposed by Zhang is used [9], and based on this method; a serendipity triangular patch with four-node is presented. Case studies have been made to investigate the effect of the location of the middle node of the serendipity patch on accuracy, and an optimal location is determined. A theoretical analysis validating the optimal location is also given with a new form of polar coordinate transformation. This system is very similar to the conventional polar system, but its implementation is simpler than the conventional polar system and also performs efficiently. With our method, the weakly singular boundary integrals in the regular or irregular elements can be accurately and effectively calculated. And our method can be also applied to the patch with large angles at the source point. Numerical examples are presented to validate the proposed method. Results demonstrate the accuracy and efficiency of our method.

This paper is organized as follows. Detailed description of the serendipity triangular patch and the coordinate system with new form are described in Section 2. In Section 3, the effect of the middle node's location in the serendipity triangular patch is introduced. Numerical examples are given in Section 4. The paper ends with conclusions in Section 5.

2. Four-node serendipity triangular patch

2.1 Four-node serendipity triangular patch

In this section, we study a serendipity triangular patch obtained through the element subdivision.

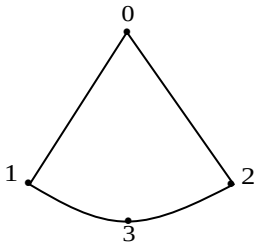

Figure 1. Four-node serendipity triangular patch.

The serendipity triangular patch is as shown in Fig. 1, the following symbols are defined:

0——the source point;

3——the middle node;

0, 1, 2, 3——serendipity patch node;

In the serendipity patch, the distance between point 0 and point 3 is equal to the length of radius of the sphere which is centered at the source point. And the length of radius we can obtain in [9]. For the patches containing source point, the coordinate transformation is used to eliminate the singularities.

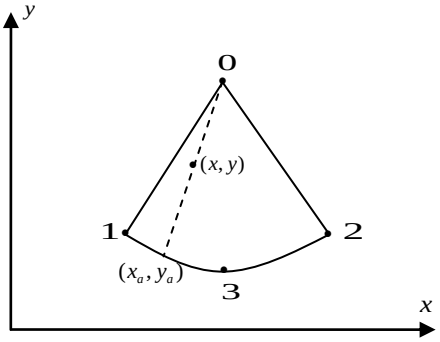

Figure 2. The coordinate transformation of serendipity triangular patch.

2.2 coordinate transformation

Considering the weakly singular integral over a patch as shown in Fig. 2, the following boundary integral can be represented as

$$I = \int_s \frac{f(y,r)}{r}\phi(x)dS \tag{1}$$

where y and x are referred to as the source point and the field point, respectively, r is the distance between y and x, f is a well-behaved function, and $\phi(x)$ is a shape function.

For this patch, to construct the local (ρ, θ) system, the following mapping is used:

$$\begin{cases} x_a = N_0 x_1 + N_1 x_2 + N_2 x_3 \\ y_a = N_0 y_1 + N_1 y_2 + N_2 y_3 \end{cases} \tag{2a}$$

In the Eq. (2a), N_0, N_1 and N_2 are the shape function of the quadratic curve.

$$\begin{aligned} N_0 &= \frac{1}{2}\theta(\theta-1) \\ N_2 &= (1+\theta)(1-\theta) \\ N_1 &= \frac{1}{2}\theta(\theta+1) \end{aligned} \tag{2b}$$

$$\begin{cases} x = x_0 + (x_a - x_0)\rho \\ y = y_0 + (y_a - y_0)\rho \end{cases} \quad \rho \in [0,1], \theta \in [-1,1] \tag{2c}$$

Combining Eq. (2a), 2(b) and (2c), the coordinate transformation can be written as:

$$\begin{cases} x = x_0 + \left([N_0 x_1 + N_2 x_3 + N_1 x_2] - x_0\right)\rho \\ y = y_0 + \left([N_0 y_1 + N_2 y_3 + N_1 y_2] - y_0\right)\rho \end{cases} \tag{3}$$

Then the integral I can be written as

$$I = \int_{-1}^{1}\int_{0}^{1} \frac{f(y,r)}{r} Jb(\rho,\theta)\phi d\rho d\theta \tag{4}$$

Where $Jb(\rho,\theta)$ is the Jacobian of the transformation from the x-y system to the ρ-θ system,

$$Jb(\rho,\theta) = \rho\left[(x_a - x_0)\frac{\partial y_a}{\partial \theta} - (y_a - y_0)\frac{\partial x_a}{\partial \theta}\right] \tag{5}$$

3. The effect of the middle node's location

3.1 Changing the middle node's location

In this section, we will investigate the effect of the middle node's location on the computational

accuracy. As shown in Fig. 3, its location is changed along the direction of the source point to the middle node by using the Eq. (6).

$$\begin{aligned} x_3 &= x_q + (x_p - x_q)t \\ y_3 &= y_q + (y_p - y_q)t \\ x_q &= \frac{x_1 + x_2}{2} \qquad y_q = \frac{y_1 + y_2}{2} \end{aligned} \tag{6}$$

As both *Jb* and *r* have ρ so we can turn it off. The plot of the function $f(\theta)=Jb/r$ on the conventional triangle patch and the serendipity triangle patch is made by MATLAB. As shown in Fig. 4, we can see when t changes from 0.1 to 1.0, the plots of the function on the serendipity triangular patch is gentler than that on the conventional linear triangle patch (t=0). Thus compared with conventional triangle patch, high accuracy results can be obtained with less Gaussian quadrature points by using the proposed serendipity triangular patch.

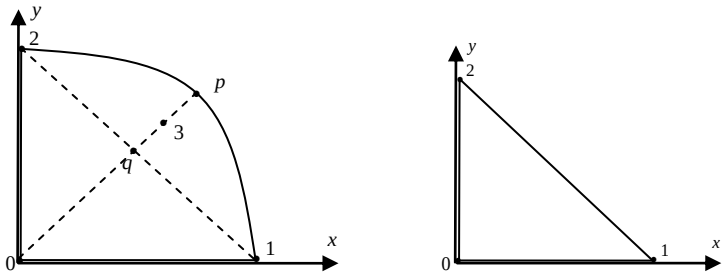

(a) (b)

Figure 3. (a) The location of the middle node in the serendipity triangular patch. (b) Conventional linear triangle patch.

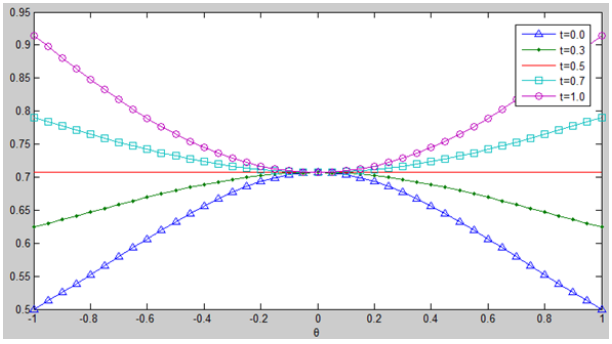

Figure 4. The plots of function *Jb/r*.

3.2 The triangle patch with large angles

In this section, the patches with large angles at the source point obtained through element subdivision are introduced. And there are some difficulties on the integrals of the angular direction in these patches.

Using Eq. (3) and Eq. (5), the Eq. (7) can be obtained.

$$\begin{aligned} f(\theta) &= \frac{Jb(\rho,\theta)}{r(\rho,\theta)} \\ &= \frac{\rho\left[(x_a - x_0)\frac{\partial y_a}{\partial \theta} - (y_a - y_0)\frac{\partial x_a}{\partial \theta}\right]}{\rho\sqrt{(x_a - x_0)^2 + (y_a - y_0)^2}} = \frac{g(\theta)}{r_1} \end{aligned} \tag{7a}$$

$$g(\theta) = (x_a - x_0)\frac{\partial y_a}{\partial \theta} - (y_a - y_0)\frac{\partial x_a}{\partial \theta} \tag{7b}$$

$$\begin{aligned} g'(\theta) &= (x_a - x_0)\frac{\partial^2 y_a}{\partial \theta^2} - (y_a - y_0)\frac{\partial^2 x_a}{\partial \theta^2} + \frac{\partial x_a}{\partial \theta}\frac{\partial y_a}{\partial \theta} - \frac{\partial x_a}{\partial \theta}\frac{\partial y_a}{\partial \theta} \\ &= (x_a - x_0)(y_1 + y_2 - 2y_3) - (y_a - y_0)(x_1 + x_2 - 2x_3) \end{aligned} \tag{7c}$$

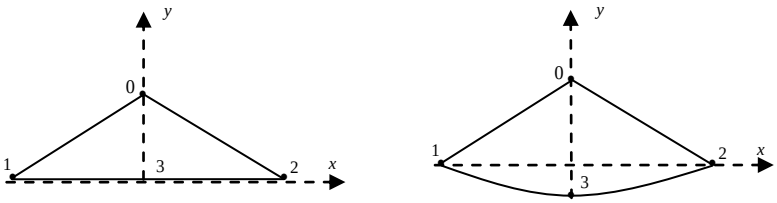

(a) (b)

Figure 5. (a) Conventional linear triangle patch; (b) serendipity triangular patch.

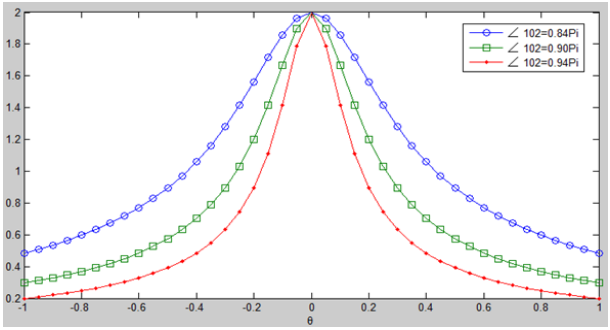

Figure 6. The plots of function *Jb/r*.

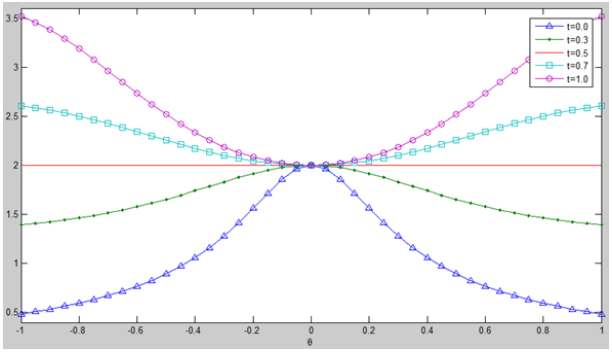

Figure 7. The plots of function *Jb/r*.

The conventional linear triangle patch as shown in Fig. 5(a), when the angle $\angle 102$ takes different values, the plots of the Eq. (7a) have been made by MATLAB. And r_1 is the distance between the source point to the point of the edge 12. As shown in Fig. 6, when the angle increase gradually, the plots of function $f(\theta)=Jb(\rho,\theta)/r$ are becoming steeper and steeper and the change of r_1 become more and more acutely. When r_1 is close to zero, the near singularity in $f(\theta)$ can be clearly seen from Fig. 6.

If the serendipity triangular patch as shown in Fig. 5(b) is used to substitute the conventional linear triangular patch, when the angle $\angle 102$ is equal to 0.84π, the plots of the function $f(\theta)=Jb(\rho, \theta)/r$ are shown in Fig. 7. It can be clearly seen that the curve in the plot become gentler and gentler when t is changed close to 0.5. So when evaluating the function $f(\theta)$, more accurate results can be obtained by using the serendipity triangular patch.

3.3 The optimal location of the middle node

In this section, the best location of the middle node is found when t is equal to 0.5. The theoretical analysis is given to verify that. And more details of the theoretical analysis are as follows.

The Eq. (3) can be written as the form of the Eq. (8).

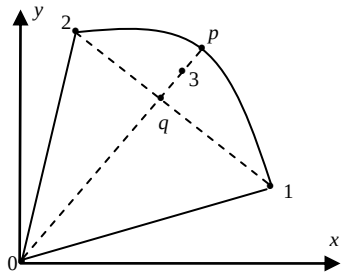

Figure 8. The location of the middle node in the serendipity triangular patch.

$$x = x_0 + (a_1\theta^2 + b_1\theta + c_1)\rho$$
$$y = y_0 + (a_2\theta^2 + b_2\theta + c_2)\rho$$
$$\frac{\partial x}{\partial \rho} = a_1\theta^2 + b_1\theta + c_1 \qquad \frac{\partial x}{\partial \theta} = (2a_1\theta + b_1)\rho \tag{8a}$$
$$\frac{\partial y}{\partial \rho} = a_2\theta^2 + b_2\theta + c_2 \qquad \frac{\partial y}{\partial \theta} = (2a_2\theta + b_2)\rho$$

$$a_1 = 0.5x_1 + 0.5x_2 - x_3 \qquad a_2 = 0.5y_1 + 0.5y_2 - y_3$$
$$b_1 = -0.5x_1 + 0.5x_2 \qquad b_2 = -0.5y_1 + 0.5y_2 \tag{8b}$$
$$c_1 = x_3 - x_0 \qquad c_2 = y_3 - y_0$$

From the element subdivision, we can obtain that the line segment 03 is perpendicular to line segment 12, and the edges 02, 01, and 0*p* have the same length *R* obtained by element subdivision [9]. In order to conveniently calculate the coordinate of the point *p*, the source point is placed in (0, 0). The coordinate of the point *p* and point 3 can be obtained by Eq. (9) and as shown in Eq. (10).

$$\begin{aligned}&(x_p - x_0)(x_2 - x_1) + (y_p - y_0)(y_2 - y_1) = 0\\ &(x_p - x_0)^2 + (y_p - y_0)^2 = (x_1 - x_0)^2 + (y_1 - y_0)^2\\ &= (x_2 - x_0)^2 + (y_2 - y_0)^2 = R^2\end{aligned} \tag{9}$$

$$x_p = x_0 + \frac{y_2 - y_1}{x_1 - x_2}\frac{R}{\sqrt{1 + (\frac{y_2 - y_1}{x_1 - x_2})^2}}$$
$$y_p = y_0 + \frac{R}{\sqrt{1 + (\frac{y_2 - y_1}{x_1 - x_2})^2}} \tag{10a}$$

$$x_3 = \frac{x_1 + x_2}{2} + (x_p - \frac{x_1 + x_2}{2})t$$
$$y_3 = \frac{y_1 + y_2}{2} + (y_p - \frac{y_1 + y_2}{2})t \tag{10b}$$

$$\begin{aligned}r^2 &= (x - x_0)^2 + (y - y_0)^2 = x^2 + y^2\\ &= (a_1^2 + a_2^2)\theta^4 + (2a_1b_1 + 2a_2b_2)\theta^3 + (2a_1c_1 + 2a_2c_2 + b_1^2 + b_2^2)\theta^2\\ &+ (2b_1c_1 + 2b_2c_2)\theta + c_1^2 + c_2^2\end{aligned}$$
$$Jb^2 = (\frac{\partial x}{\partial \rho}\frac{\partial y}{\partial \theta} - \frac{\partial y}{\partial \rho}\frac{\partial x}{\partial \theta})^2$$
$$= \left\{\begin{array}{l}(a_2b_1 - a_1b_2)^2\theta^4 + (2a_2b_1 - 2a_1b_2)(2a_2c_1 - 2a_1c_2)\theta^3\\ \quad + [2(a_2b_1 - a_1b_2)(c_1b_2 - c_2b_1) + (2a_2c_1 - 2a_1c_2)^2]\theta^2\\ \quad + 2(2a_2c_1 - 2a_1c_2)(c_1b_2 - c_2b_1)\theta + (c_1b_2 - c_2b_1)^2\end{array}\right\}\rho^2 \tag{11}$$

Using Eq. (8a) and Eq. (8b), the Eq. (11) can be obtained. As the line segment 12 is perpendicular to the line segment 0*p* and the slope of the line *pq* is equal to that of the line 03. The Eq. (12) can be obtained.

$$\begin{aligned}&2a_1b_1 + 2a_2b_2 = 0\\ &2b_1c_1 + 2b_2c_2 = 0\\ &2a_2c_1 - 2a_1c_2 = 0\end{aligned} \tag{12}$$

Using Eq. (12), Eq. (11) can be written as:

$$Jb^2 = [(a_2b_1 - a_1b_2)^2\theta^4 + 2(a_2b_1 - a_1b_2)(c_1b_2 - c_2b_1)\theta^2 + (c_1b_2 - c_2b_1)^2]\rho^2$$
$$r^2 = [(a_1^2 + a_2^2)\theta^4 + (2a_1c_1 + 2a_2c_2 + b_1^2 + b_2^2)\theta^2 + c_1^2 + c_2^2]\rho^2$$

And Eq. (11) can be further written as:

$$\begin{aligned}Jb^2 &= (a_2b_1 - a_1b_2)^2\theta^4 + 2(a_2b_1 - a_1b_2)(c_1b_2 - c_2b_1)\theta^2 + (c_1b_2 - c_2b_1)^2\\ &= \alpha^2(a_2b_1 - a_1b_2)^2[\theta^2 + \frac{c_1b_2 - c_2b_1}{a_2b_1 - a_1b_2}]^2\end{aligned}$$
$$r^2 = \alpha^2[(a_1^2 + a_2^2)\theta^4 + (2a_1c_1 + 2a_2c_2 + b_1^2 + b_2^2)\theta^2 + c_1^2 + c_2^2]$$
$$= \alpha^2\left\{\begin{array}{l}(a_1^2 + a_2^2)[\theta^2 + \frac{(2a_1c_1 + 2a_2c_2 + b_1^2 + b_2^2)}{2(a_1^2 + a_2^2)}]^2\\ +(c_1^2 + c_2^2) - \frac{(2a_1c_1 + 2a_2c_2 + b_1^2 + b_2^2)^2}{4(a_1^2 + a_2^2)}\end{array}\right\} \tag{13}$$

$$M = 4(c_1^2 + c_2^2)(a_1^2 + a_2^2) - (2a_1c_1 + 2a_2c_2 + b_1^2 + b_2^2)^2 \tag{14}$$

$$x_1^2 = R - y_1^2 \qquad x_2^2 = R - y_2^2 \tag{15}$$

Substitute the parameter *a1*, *a2*, *b1*, *b2*, *c1*, *c2* and Eq. (15) into Eq. (14) and Eq. (16), respectively. Calculate it in MAPLE 15 when t is equal to 0.5, M=0 and N=0 can be easily obtained. So t=0.5 is a common root of the equation $M(t)$=0 and $N(t)$=0.

$$\begin{aligned} N &= 2(c_1b_2 - c_2b_1)(a_1^2 + a_2^2) \\ &-(2a_1c_1 + 2a_2c_2 + b_1^2 + b_2^2)(a_2b_1 - a_1b_2) \end{aligned} \tag{16}$$

That is to say, when t is equal to 0.5, the Eq. (17) is workable and the ratio of $Jb(\rho,\theta)/r$ has nothing to do with ρ and θ. And the ratio A can be expressed as follows in Eq. (18).

$$\begin{cases} \dfrac{c_1b_2 - c_2b_1}{a_2b_1 - a_1b_2} = \dfrac{(2a_1c_1 + 2a_2c_2 + b_1^2 + b_2^2)}{2(a_1^2 + a_2^2)} \\ (c_1^2 + c_2^2) - \dfrac{(2a_1c_1 + 2a_2c_2 + b_1^2 + b_2^2)^2}{4(a_1^2 + a_2^2)} = 0 \end{cases} \tag{17}$$

$$A = \frac{(a_2b_1 - a_1b_2)^2}{(a_1^2 + a_2^2)} \tag{18}$$

With the detailed description above, it can be clearly seen that our method has obvious advantages over conventional method.

4. Numerical examples

To evaluate the effectiveness and accuracy of our method, in this section, several comparisons are made between our method and the conventional method for planar element and curved surface element. For the purpose of error estimation, relative error is defined as follows:

$$\text{Relative Error} = \left| \frac{I_n - I_e}{I_e} \right| \tag{19}$$

where I_n is the numerical solution, and I_e is the exact solution of the integral.

We consider the numerical evaluation of the integral

$$I = \int_\Gamma \frac{1}{r} \phi d\Gamma \tag{20}$$

In Eq. (20), where Γ is an arbitrary boundary element and ϕ is a shape function of the element. And in all the numerical examples, the above coordinate transformation is used to remove singularities in the patches which contain the source point, while the remaining regular quadrilateral and triangular patches are respectively evaluated by the standard Gaussian quadrature. The number of the Gaussian points m is determined by [10-12].

4.1 Examples of serendipity triangle patch

In this example, we study the influence of the middle node's location on the computational accuracy in our method when the source point is fixed. As shown in Fig. 9, three vertexes of the patch located at (0, 1, 0), (-2, 0, 0) and (2, 0, 0), respectively. In each case, the source point is fixed at (0, 1, 0), and the middle node 3 is determined by an offset parameter $t, 0 \le t \le 1$, using the following equation :

$$\begin{aligned} x_3 &= \frac{x_1 + x_2}{2} + (x_p - \frac{x_1 + x_2}{2})t \\ y_3 &= \frac{y_1 + y_2}{2} + (y_p - \frac{y_1 + y_2}{2})t \end{aligned} \tag{10b}$$

$$x_p = 0.0 \qquad y_p = 1.0 - \frac{\sqrt{5}}{\sqrt{1 + (\frac{y_2 - y_1}{x_1 - x_2})^2}} = 1.0 - \sqrt{5}$$

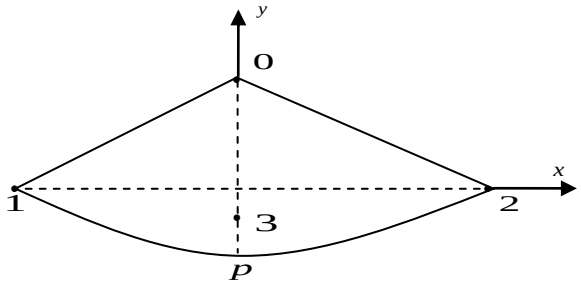

Figure 9. The location of the middle point of the serendipity triangular patch.

Table 1: Gaussian points number used by linear and serendipity patch in case of equivalent accuracy.

	Gaussian points number			Relative Error
	(angular direction)	(radius direction)	total	
Conventional method (t=0.0)	14	5	70	7.14e-007
Our method (t=0.3)	10	5	50	2.34e-007
Our method (t=0.5)	2	5	10	3.33e-016
Our method (t=0.7)	7	5	35	2.86e-008
Our method (t=1.0)	7	5	35	9.97e-007

Table 2: accuracy obtained by linear and serendipity patch in case of equivalent Gaussian sample points.

	Gaussian points number			Relative Error
	(angular direction)	(radius direction)	total	
Conventional method (t=0.0)	7	5	35	8.43e-004
Our method (t=0.3)	7	5	35	2.31e-005
Our method (t=0.5)	7	5	35	3.33e-016
Our method (t=0.7)	7	5	35	2.86e-008
Our method (t=1.0)	7	5	35	9.97e-007

The accuracy obtained by both our method and the conventional method and the number of the Gaussian sample points used are listed in Table 1 and Table 2. It is seen that to obtain the same level of accuracy, our method needs much fewer sample points, and thus, considerably increases the computational efficiency. And as illustrated in Table 1 and Table 2, from the numerical solutions obtained we can find that when t = 0.5, we can obtain the highest accuracy with the fewest Gaussian sample points.

4.2 Examples of triangle element with large-angle

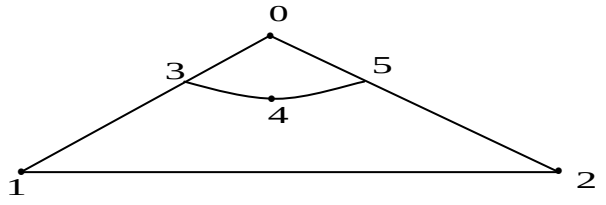

Figure 10. Subdivisions of planar triangular element with our method.

In this part, we study the numerical evaluation of the triangle element in our method when t = 0.5. Three vertexes of the element are located at (0, 1, 0), (-4, 0, 0) and (4, 0, 0), respectively. And the source point is fixed at (0, 1, 0). Through adaptive element subdivision [9], the element is subdivided two patches as shown in Fig. 10. And the angle at the source point is approximate equal to 0.84π. The coordinate of point 3, 4 and 5 can be calculated by using Eq. (10b).

The accuracy obtained by both our method and the conventional method and the number of the Gaussian sample points used are listed in Table 3. It can be seen that to obtain the same level of accuracy, our method needs much fewer sample points, and thus, considerably increases the computational efficiency.

Table 3: Numerical evaluation for planar triangular element.

	Gaussian points number	Relative Error	Gaussian points number	Relative Error
Conventional method	55	1.68e-003	130	9.05e-007
Our method (t=0.5)	54	8.11e-006	87	5.60e-007

4.3 Examples of planar element

In this example, we study the numerical evaluation of the planar quadrilateral element in our method when t = 0.5. The vertexes of the element are located at (1, 1, 0), (-1, 1, 0), (-1, -1, 0) and (1, -1, 0), respectively. And the source point is fixed at (0, -0.9, 0). As shown in Fig. 13, the source points are very close to the edge. Through adaptive element subdivision [9], the element is subdivided into a few patches as shown in Fig. 11(b).

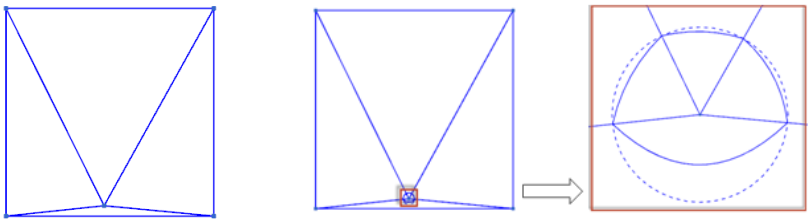

(a) the conventional method (b) Our method

Figure 11. Subdivisions of planar quadrilateral element with our method.

Table 4: Numerical evaluation for planar quadrilateral element.

	Gaussian points number	Relative Error	Gaussian points number	Relative Error
Conventional method	672	3.01e-004	1664	7.79e-007
Our method (t=0.5)	652	3.95e-006	872	4.81-007

The accuracy obtained by both our method and the conventional method and the number of the Gaussian sample points used are listed in Table 4. It is seen that when the number of Gaussian sample points used is the same, the accuracy obtained by our method is higher than that by the conventional method. And to obtain the same level of accuracy, our method needs much fewer sample points. The effectiveness and accuracy of our method are demonstrated again.

5. Conclusions

In this paper, a serendipity triangle patch with four-node is introduced for calculating the singular integrals in the BIE. By theoretical analysis and numerical experiment, the optimal location of the middle node of the serendipity patch has been found for the highest accuracy and efficiency. From the numerical examples, it has been demonstrated that our method can achieved much better accuracy than the conventional method with equivalent number of Gaussian sample points. On the other hand, to obtain the same level of accuracy, our method requires

much fewer sample points, and thus, considerably increases the computational efficiency. Extending our method to compute curved surface element and 3D nearly singular integral is straightforward and ongoing.

Acknowledgement

This work was supported by National Science Foundation of China (Grant No.11172098 and No. 11472102) , and in part by Open Research Fund of Key Laboratory of High Performance Complex Manufacturing, Central South University (Grant No. Kfkt2013-05).

References

[1] Kane JH. Boundary Element Analysis in Engineering Continuum Mechanics. Prentice-Hall: Englewood Cliffs, NJ, 1994.

[2] Klees R. Numerical calculation of weakly singular surface integrals. J Geodesy 1996; 70(11): 781-797.

[3] Telles JCF. A self-adaptive co-ordinate transformation for efficient numerical evaluation of general boundary element integrals. International Journal for Numerical Methods in Engineering 1987; 24: 959-973.

[4] Scuderi L.On the computation of nearly singular integrals in 3D BEM collocation. Int J Numer Methods Eng 2008; 74: 1733–1770.

[5] Hayami K. Variable transformations for nearly singular integrals in the boundary element method[J]. Publications of the Research Institute for Mathematical Sciences 2005; 41(4): 821-842.

[6] Johnston BM, Johnston PR, Elliott D. A new method for the numerical evaluation of nearly singular integrals on triangular elements in the 3D boundary element method. J Comput Appl Math 2013; 245: 148–161.

[7] Junjie Rong, Lihua Wen and Jinyou Xiao. Efficiency improvement of the polar coordinate transformation for evaluating BEM singular integrals on curved elements. Engineering Analysis with Boundary Elements 2014; 38: 83-93.

[8] Guizhong Xie, Fenglin Zhou, Jianming Zhang, Xingshuai Zheng and Cheng Huang. New variable transformations for evaluating nearly singular integrals in 3D boundary element method. Engineering Analysis with Boundary Elements, 2013; 37: 1169-1178.

[9] Jianming Zhang, Chenjun Lu and Xiuxiu Zhang. An adaptive element subdivision method for evaluation of weakly singular integrals in 3D BEM. Engineering Analysis with Boundary Elements 2015; 51: 213-219.

[10]Gao XW, Davies T G. Adaptive integration in elasto−plastic boundary element analysis. Journal of the Chinese institute of engineers 2000; 23(3): 349-356.

[11]Bu S, Davies TG. Effective evaluation of non-singular integrals in 3D BEM. Advances in Engineering Software 1995; 23(2): 121-128.

[12]Lachat JC, Watson JO. Effective numerical treatment of boundary integral equations: A formulation for three-dimensional elastostatics. International Journal for Numerical Methods in Engineering 1976; 10(5): 991-1005.